Frictional Drag and Electrical Manipulation of Recombinant Proteins in Polymer-Supported Membranes

Motomu Tanaka,*[,†,§] Joachim Hermann,[†,||] Ilka Haase,[‡,⊥] Markus Fischer,[‡,⊥] and Steven G. Boxer[||]

Departments of Physics and Chemistry, Technical University of Munich, D-85748 Garching, Germany, Institute of Physical Chemistry, University of Heidelberg, D-69120 Heidelberg, Germany, and Department of Chemistry, Stanford University, Stanford, California 94305-5080

Received September 26, 2006. In Final Form: February 8, 2007

We establish a lipid monolayer supported by a polymer interface that offers advantages over conventional solid-supported membranes for determining the frictional drag at the membrane−protein interface as well as for electric field manipulation of membrane-anchored proteins. Polymer-supported monolayers with functional lipid anchors allow for the specific docking of His-tagged green fluorescent protein variants (His-EGFP and His-DsRed tetramer) onto the membrane surface at a defined surface density. In the first part, we measure the lateral diffusion coefficients of lipids and proteins and calculate the frictional drag at the protein−membrane interface. The second part deals with the electric field-induced accumulation of recombinant proteins on a patterned surface. The mean drift velocity of proteins, which can be obtained analytically from the shape of the steady-state concentration gradient, can be controlled by tuning the interplay of electrophoresis and electroosmosis. The results demonstrate the potential of such molecular constructs for the local functionalization of solid substrates with membrane-associated proteins.

Introduction

Phospholipid membranes deposited on planar substrates (supported membranes) have been intensively and widely employed as models of cell surfaces to study various cellular functions, such as the immune response and cell adhesion processes.[1−4] Compared to free-standing black lipid membranes and spherical lipid vesicles, supported membranes have significant advantages because of their ability to coat macroscopically large surfaces (on the order of square centimeters), their excellent mechanical stability, and their planar geometry that is ideally suited to surface-sensitive analytical methods. Owing to their amphiphilic property, phospholipids form monolayers on hydrophobic substrates and bilayers on some hydrophilic substrates, and these can be utilized as quasi-2D matrices in which peripheral and integral proteins can be accommodated.

To confine supported membranes and membrane-associated proteins in a defined geometry, micropatterning of supported membranes has been developed by several groups using diffusion barriers,[5] photochemical cross-linking of lipid anchors,[6] microcontact printing of membranes,[7] and microfluidic channels.[8,9] More recently, we further achieved selective deposition of native biomembranes (human red blood cells and microsomes) on prepatterned polymer templates.[10] Components associated with supported membranes can be reorganized by application of an electric field parallel to the plane of the membrane. To date, this technique has mainly been used to accumulate charged lipid molecules,[11,12] DNA bound to the membrane,[13,14] or tethered vesicles.[15,16] However, there have been only a few reports on the accumulation of membrane-associated proteins and native cell membranes.[17−20]

In spite of substantial progress, solid-supported membranes still suffer from several fundamental disadvantages. Charged lipid tracer molecules exist both in proximal (the lower leaflet) and distal monolayers (the upper leaflet), but the frictional drag experienced by each monolayer is different. The thickness of the water reservoir between the membrane and substrate is known to be around 5 −20 Å but is ill-defined. Because most electrical manipulations need to be carried out at low salt concentrations below 10 mM, the Debye screening length (corresponding to the thickness of the electrochemical double layer) is often comparable or even higher than the membrane−substrate distance.

One possible solution is to graft a hydrophobic monolayer covalently onto a solid substrate and deposit the distal layer onto this substrate.[21] However, chemical grafting of alkyl chains onto

* Corresponding author. E-mail: tanaka@uni-heidelberg.de. Fax: +49-6221544918.

† Department of Physics, Technical University of Munich.

‡ Department of Chemistry, Technical University of Munich.

§ University of Heidelberg.

|| Stanford University.

⊥ Present address: Institute of Biochemistry and Food Chemistry, University of Hamburg, D-20146 Hamburg, Germany.

(1) Brian, A. A.; McConnell, H. M. *Proc. Natl. Acad. Sci. U.S.A.* **1984**, *81*, 6159.

(2) Chan, P.; Lawrence, M. B.; Dustin, M. L.; Ferguson, L. M.; Golan, D. E.; Springer, T. A. *J. Cell Biol.* **1991**, *10*, 245.

(3) Sackmann, E. *Science* **1996**, *271*, 43.

(4) Groves, J. T.; Boxer, S. G. *Acc. Chem. Res.* **2002**, *35*, 149.

(5) Groves, J. T.; Ulman, N.; Boxer, S. G. *Science* **1997**, *275*, 651.

(6) Morigaki, K.; Baumgart, T.; Offenhausser, A.; Knoll, W. *Angew. Chem., Int. Ed.* **2001**, *40*, 172.

(7) Hovis, J. S.; Boxer, S. G. *Langmuir* **2000**, *16*, 894.

(8) Janshoff, A.; Künneke, S. *Eur. Biophys. J.* **2000**, *29*, 549.

(9) Yang, T.; Baryshnikova, O. K.; Mao, H.; Holden, M. A.; Cremer, P. S. *J. Am. Chem. Soc.* **2003**, *125*, 4779.

(10) Tanaka, M.; Wong, A. P.; Rehfeldt, F.; Tutus, M.; Kaufmann, S. *J. Am. Chem. Soc.* **2004**, *126*, 3257.

(11) Stelzle, M.; Mielich, R.; Sackmann, E. *Biophys. J.* **1992**, *63*, 1346.

(12) Groves, J. T.; Boxer, S. G.; McConnell, H. M. *Proc. Natl. Acad. Sci. U.S.A.* **1997**, *25*, 13390.

(13) Olson, D. J.; Johnson, J. M.; Partel, P. D.; Shaqfeh, E. S. G.; Boxer, S. G.; Fuller, G. G. *Langmuir* **2001**, *17*, 7396.

(14) Galneder, R.; Kahl, V.; Arbuzova, A.; Rebecchi, M.; Rädler, J. O.; McLaughlin, S. *Biophys. J.* **2001**, *80*, 2298.

(15) Yoshina-Ishii, C.; Boxer, S. G. *J. Am. Chem. Soc.* **2003**, *125*, 3696.

(16) Yoshina-Ishii, C.; Boxer, S. G. *Langmuir* **2006**, *22*, 2384.

(17) Poo, M.-M.; Robinson, K. R. *Nature* **1977**, *265*, 602.

(18) McLaughlin, S.; Poo, M.-M. *Biophys. J.* **1981**, *34*, 85.

(19) Grogan, M. J.; Kaizuka, Y.; Conrad, R. M.; Groves, J. T.; Bertozzi, C. R. *J. Am. Chem. Soc.* **2005**, *127*, 14383.

(20) Ryan, T. A.; Myers, J.; Holowka, D.; Baird, B.; Webb, W. W. *Science* **1988**, *239*, 61.

(21) Merkel, R.; Sackmann, E.; Evans, E. *J. Phys. France* **1989**, *50*, 1535.

10.1021/la0628219 CCC: $37.00
Published on Web 04/05/2007

solid substrates results in the formation of highly ordered crystalline-like hydrocarbon chains. The lateral mobility of lipid molecules in a distal layer is found to be considerably reduced because of significant frictional drag between the crystalline-like hydrocarbon chains and the distal monolayer.[21,22] This can be partially overcome by grafting a self-assembled alkyl monolayer with a lower lateral density; however, the quantitative control or determination of the fractional drag contribution from the lateral density of alkyl chains is very difficult. This may be due to the fact that the lower grafting density does not correspond to the uniform dilution of alkyl chains but instead results in a monolayer with numerous local defects whose sizes are often found to be as large as tens of micrometers. Thus, a common technique for determining lateral diffusion coefficients (fluorescence recovery after photobleaching or FRAP) that detects the diffusion of tracer molecules on a length scale on the order of 10 micrometers or the electrically driven drift of molecules that is detected on the length scale of several tens to hundreds of micrometers is not suitable. Also, quantitative measurements of the frictional drag and the drift of lipids and proteins under external fields have not been reported.

To offer hydrophobic but lower-friction environments to lipid membranes, we deposit phospholipids monolayers on hydrophobic polymer supports.[23,24] The surface of polymer supports, consisting of isopentyl cellulose cinnamate (IPCC), uniformly displays disordered (and thus noncrystalline) alkyl chains, which enables the reduction of friction against the lipid monolayer. Isopentyl side chains are covalently linked to the cellulose backbone at high density (~3 alkyl chains per glucose unit) but always remain disordered owing to their branched structure. Previously, we demonstrated that it is possible to deposit homogeneous, defect-free lipid monolayers onto 10 nm thick IPCC supports (i.e., thick enough to isolate the distal monolayer from the underlying substrate)[25] while keeping the lateral diffusion constants of lipids more than 10 times higher than those on crystalline-like monolayers.[21,22] As well-defined proteins, we selectively couple two types of genetically modified recombinant proteins with histidine tags (monomeric His-EGFP with MW = 28.1 kDa and tetrameric His-DsRed with MW = 107.6 kDa) to lipids functionalized with nitrilotriacetic acid (NTA) head groups. The use of protein docking via specific lipid anchors enables us to quantitatively control the lateral density of proteins on the surface. In the first part, we measure the lateral diffusion coefficients of lipids and proteins by fluorescence recovery after photobleaching (FRAP). Taking the Saffman−Delbrück theory[26,27] modified by Evans and Sackmann,[28] we calculate the frictional drag between recombinant proteins and polymer-supported lipid monolayers. In the second part, we accumulate these recombinant proteins by applying tangential electric fields. From an analysis of the shape of the steady-state protein/lipid concentration gradient, we deduce the mean drift velocity of tethered proteins. The electrically driven accumulation of proteins and lipids can be described by the interplay of electrophoresis and electroosmosis, which allows us to accelerate/deaccelerate protein drifts.

Materials and Methods

Lipids, Recombinant Proteins, and Buffers. Zwitterionic lipid 1-stearoyl-2-oleoyl-*sn*-glycero-3-phosphocholine (SOPC) was used as a matrix lipid. To introduce negative charges onto the membrane, 1-stearoyl-2-oleoyl-*sn*-glycero-3-[phospho-L-serine] (SOPS) was used. To anchor histidine-tagged recombinant proteins, 1,2-dioleoyl-*sn*-glycero-3-[*N*-(5-amino-1-carboxypentyl) iminodiacetic acid) succinyl] (DOGS-NTA) was doped into the matrix lipids. All of the lipids were purchased from Avanti Polar Lipids (Alabaster, AL). Texas red (1,2-dihexadecanoyl-*sn*-glycero-3-phosphoethanolamine, triethylammonium salt) (Molecular Probes, Leiden, The Netherlands) was doped as a negatively charged lipid probe in order to monitor the lateral diffusivity and electrophoretic mobility of lipid molecules. Two types of recombinant proteins with six histidine residues have been used: green fluorescent protein (His-EGFP) and red fluorescent protein (His-DsRed) (Supporting Information). The standard buffer contains 10 mM Na_2HPO_4 and 100 mM NaCl (phosphate buffer), 10 mM $NiCl_2$ (nickel buffer), or 50 mM EDTA (ethylenediaminetetraacetic acid, EDTA buffer). All other chemicals were purchased from Fluka (Neu Ulm, Germany) and were used without further purification.

Sample Preparation. Polymer-supported membranes were deposited on clean glass slides (Karl Hecht KG, Sondheim). Prior to the deposition of polymer supports, the glass slides were hydrophobized by grafting octadecyltrimethoxysilane (ABCR, Karlsruhe) monolayers.[29] Langmuir−Blodgett films of isopentylcellulose cinnamate (IPCC) were deposited onto hydrophobic substrates at a constant pressure of 18 mN/m and $T = 293$ K. As reported elsewhere,[25] IPCC has degrees of substitution (DS) of 2.9 for isopentyl groups and 0.1 for cinnamoyl groups. The cinnamoyl side groups of the polymers were crosslinked by irradiation with a 500 W Hg-(Xe) lamp (Oriel Instruments, Stratford, CT) for 4 min. The incident light from the lamp was reflected by an aluminum mirror to cut off deep UV light ($\lambda < 220$ nm) to avoid photoablation. After photocrosslinking, the film is stable against treatment with organic solvents such as chloroform and ethanol.[25] Lipid monolayers were deposited on the hydrophobic, crosslinked IPCC cushion by exchange of solvent from ethanol to aqueous buffer.[25,30] The flow chamber was filled with lipid mixtures dissolved in ethanol (0.5 mg/mL), and the lipid monolayer was formed by diluting the ethanol solution with nickel buffer. All of the experiments were carried out at $T = 293$ K.

Fluorescence Microscopy and Measurements of Diffusion Constants. Fluorescence images of lipid monolayers and membrane-anchored proteins were recorded with an Zeiss Axiovert 200 (Zeiss, Göttingen) with an Orca ER cooled CCD camera (Hamamatsu Photonics, Herrsching) or with a Nikon TE300 (Nikon) with a Pentamax GIII CCD camera (Roper scientific). The passive diffusion constants of lipids were measured by fluorescence recovery after photobleaching (FRAP).[31,32] As described previously,[25] a 1 W argon ion laser (Innova 70, Coherent, Santa Clara, CA) was used as the light source for bleaching as well as for the observation of fluorescence recovery. The bleaching spot had a radius of $r = 4.7$ μm.

In the case of a 2D membrane with a circular concentration profile, the intensity profile integrated over the bleaching area can be represented according to the analytical method reported by Soumpasis.[32] By taking the radius of the bleaching spot to be $r = 4.7$ μm and the characteristic time constant τ obtained from the analytical fit, one can deduce the diffusion coefficient D, and the fraction of mobile species can be calculated from the relative fluorescence recovery R.

Electrical Manipulation of Lipids and Proteins. Once a lipid monolayer was formed on a polymer support, diffusion barriers were established by scratching the film with metal tweezers.[5,33,34]

(22) Sigl, H.; Brink, G.; Schulze, M.; Wegner, G.; Sackmann, E. *Eur. Biophys. J.* **1997**, *25*, 249.
(23) Tanaka, M.; Sackmann, E. *Nature* **2005**, *437*, 656.
(24) Tanaka, M. *MRS Bull.* **2006**, *31*, 513.
(25) Hillebrandt, H.; Tanaka, M.; Sackmann, E. *J. Phys. Chem. B* **2002**, *106*, 477.
(26) Saffman, P. G.; Delbruck, M. *Proc. Natl. Acad. Sci. U.S.A.* **1975**, *72*, 3111.
(27) Hughes, B. D.; Pailthorpe, B. A.; White, L. R. *J. Fluid. Mech.* **1981**, *110*, 349.
(28) Evans, E.; Sackmann, E. *J. Fluid. Mech.* **1988**, *194*, 553.
(29) Hillebrandt, H.; Tanaka, M. *J. Phys. Chem. B* **2001**, *105*, 4270.
(30) Miller, C.; Cuendet, P.; Grätzel, M. *J. Electroanal. Chem.* **1990**, *278*, 175.
(31) Axelrod, D.; Koppel, D. E.; Schlessinger, E.; Elson, E.; Webb, W. W. *Biophys. J.* **1976**, *16*, 1055.
(32) Soumpasis, D. M. *Biophys. J.* **1983**, *16*, 95.
(33) Groves, J. T.; Boxer, S. G. *Biophys. J.* **1995**, *69*, 1972.
(34) Groves, J. T.; Wulfing, C.; Boxer, S. G. *Biophys. J.* **1996**, *71*, 2716.

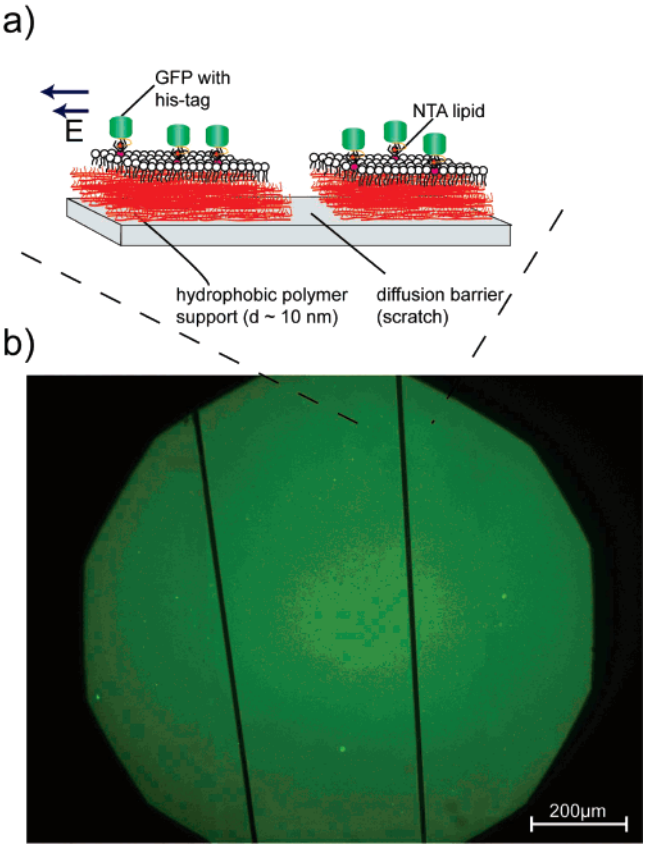

Figure 1. (a) Schematic overview and (b) fluorescence image of histidine-tagged His-EGFP variants coupled to a polymer-supported lipid monolayer, which consists of 98 mol % SOPC and 2 mol % DOGS-NTA. The lateral density of His-EGFP can roughly be estimated to be 40 nm^2.

After scratching, the sample was assembled into a sandwich with another glass slide, which was then mounted into an electrophoresis chamber.[11,34] Prior to the electric manipulation, the sample kept in nickel buffer was rinsed with Millipore water. A tangential electric field of 10 V/cm was applied between two platinum wires, which led to an accumulation of lipids or proteins on the closest diffusion barrier. It should be noted that the lipid membrane must be kept under water throughout the procedures to avoid dewetting.

Here, we consider the steady-state concentration gradient between two diffusion barriers when a tangential electric field is applied to a 2D fluid by eliminating the time-dependent terms:

$$D\frac{\partial^2 C(x,t)}{\partial x^2} + \langle v\rangle \frac{\partial C(x,t)}{\partial x} = 0 \qquad (1)$$

In our experimental system, steady state can typically be reached within 20−60 min by applying a 10 V/cm field. This equation can be solved to give

$$C(x) = A\exp\left(\frac{x}{\xi}\right) + B \qquad (2)$$

where A and B are the amplitude and the integration term, respectively. The characteristic decay length ξ enables one to calculate the mean velocity $\langle v\rangle$ using the passive diffusion constant D from FRAP measurements: $\langle v\rangle = D/\xi$.

Results and Discussion

Docking of Recombinant Proteins and Passive Lateral Diffusion. Figure 1 shows (a) a schematic overview and (b) a fluorescence image of histidine-tagged EGFP (His-EGFP) coupled to a polymer-supported lipid monolayer. Here, the lipid monolayer consists of 98 mol % SOPC and 2 mol % DOGS-NTA. From the area per lipid molecule in the fluid phase (65 Å^2),[35] the average area per Ni-NTA lipid that serves as a specific anchoring point for a protein can be roughly estimated to be 40 nm^2. As presented in Figure 1b, His-EGFP can be anchored on the monolayer homogeneously, showing no local defects at the resolution of the light microscope. All of the anchored proteins can be removed by rinsing with EDTA buffer and verifying the specific docking of histidine-tagged recombinant proteins to Ni-NTA lipids. The lateral diffusion coefficient of GFP coupled to the membrane was measured by FRAP (Figure 2), yielding a diffusion coefficient of $D = 1.5 \pm 0.1\ \mu m^2\ s^{-1}$. [The diffusion coefficients and mobile fractions presented here are the mean values from at least five independent measurements. The small errors as well as almost 100% realtive recoveries observed here confirm the homogeneities of lipid/protein distributions as well as the reproducibility of our surface functionalization.] Furthermore, almost all (96 ± 2%) of the bound GFPs are found to be freely mobile, confirming that there is no crystallization of proteins on the membrane surface. The docking of His-DsRed tetramers follows the same procedure. When the fraction of Ni-NTA lipids was 2 mol %, the sample showed homogeneous docking of His-DsRed on the polymer-supported lipid monolayer. Treatment with EDTA buffer results in the complete detachment of proteins, which confirms the specific binding of His-DsRed to Ni-NTA lipids. However, in the presence of 5 mol % DOGS-NTA (corresponding to the average lateral density of 1 NTA lipid in about 13 nm^2), the bound His-DsRed cannot be removed by treatment with EDTA buffer. This can be attributed either to the nonspecific adsorption of proteins onto the surface with high anchor densities or to the lateral crystallization of proteins.[36] FRAP experiments demonstrate that 96 ± 1% His-DsRed are mobile on the membrane with 2 mol % DOGS-NTA, exhibiting a lateral diffusion coefficient of $D = 1.4 \pm 0.05\ \mu m^2\ s^{-1}$. Interestingly, the diffusion constants of His-EGFP and His-DsRed are almost identical, in spite of a large difference in their molecular weights (28.1 kDa for monomeric His-EGFP and 107.6 kDa for tetrameric His-DsRed). This suggests that the diffusion coefficient is determined primarily by the friction between NTA lipid anchors and the surrounding SOPC matrix. As a reference, the fluorescent lipids (NBD-PE doped into the polymer-supported monolayer) give a diffusion coefficient and mobile fraction of $D = 3.2 \pm$

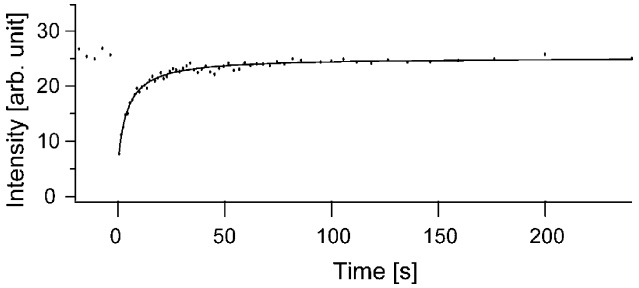

Figure 2. Recovery of fluorescence intensity after photobleaching of GFP with a short (100 ms), intensive Ar laser pulse (diameter of 9.3 μm). The membrane consists of the same components as in Figure 1. The obtained diffusion constant ($D = 1.5 \pm 0.1\ \mu m^2\ s^{-1}$) and mobile fraction (96 ± 2%) clearly indicate that the polymer support can provide the membrane-anchored GFPs with a fluid environment, where almost all of them can freely diffuse on the membrane surface.

(35) Sackmann, E. Biological Membranes Architecture and Function. In *Handbook of Biological Physics*; Lipowsky, R., Sackmann, E., Eds.; Elsevier Science: New York, 1995.

(36) Dorn, I. T.; Pawlitschko, K.; Pettinger, S. C.; Tampé, R. *Biol. Chem.* **1998**, *379*, 1151.

Table 1. Summary of Fluorescence Recovery after Photobleaching (FRAP) Experiments[a]

sample	diffusion coefficient ($\mu m^2 s^{-1}$)	mobile fraction
His-EGFP tagged to 2 mol % NTA lipid	1.5 ± 0.1	0.96 ± 0.02
His-DsRed tetramer tagged to 2 mol % NTA lipid	1.4 ± 0.05	0.96 ± 0.01
Texas red-labeled lipid (2 mol %)	3.2 ± 0.10	0.97 ± 0.01

[a] Diffusion constants and mobile fractions of lipids and proteins were calculated from the FRAP results. SOPC was used as the matrix lipid. The specific docking of histidine-tagged proteins was confirmed by complete removal upon EDTA buffer treatment. Note that 2 mol % NTA lipids (i.e., the mean area per fluorescent lipid/protein of about 40 nm^2) was chosen to confirm nonspecific adsorption and clustering of proteins. Indeed, significant nonspecific adsorption of His-DSRed was observed at an NTA lipid fraction of 5 mol %.

$0.10\ \mu m^2\ s^{-1}$ and $R = 0.97 \pm 0.01$, respectively. The results of FRAP experiments are summarized in Table 1.

Frictional Drag in Polymer-Supported Monolayers. Generally, the diffusion coefficient D is given by the Einstein relation

$$D = \frac{kT}{\lambda} \tag{3}$$

where λ is the drag coefficient. As an extension of the theory introduced by Saffman and Delbrück[26] and Hughes et al.,[27] Evans and Sackmann proposed that the drag coefficient can be given by the viscosity of the membrane η_m and the dimensionless particle radius ϵ[21,28]

$$\lambda = 4\pi\eta_m\left[\frac{1}{4}\epsilon^2 + \frac{K_1(\epsilon)}{K_0(\epsilon)}\epsilon\right] \tag{4}$$

where η_m is the 2D viscosity of a monolayer (and therefore, half of the viscosity of a free bilayer, η_{bl}) and K_0 and K_1 are modified Bessel functions of the second kind of orders 0 and 1, respectively. The dimensionless particle radius ϵ can be represented by taking the radius of a disk spanning the membrane a_p and the frictional coefficient b_s:

$$\epsilon = a_p\sqrt{\frac{b_s}{\eta_m}} \tag{5}$$

To determine the influence of the exterior solution on the interfacial drag, the dimensionless particle radius needs to be rewritten as

$$\epsilon^* = a_p\sqrt{\frac{b_s + b_\infty}{\eta_m}} \tag{6}$$

where b_∞ is the frictional drag from the semifinite bath solution. The frictional coefficient can be derived by converting the measured diffusion coefficient to the dimensionless particle mobility m:

$$m = \frac{4\pi\eta_m}{\lambda} = \frac{4\pi\eta_m D}{kT} \tag{7}$$

Previously, Merkel et al.[21] studied molecular friction in solid-supported membranes. To study the frictional coefficient between proximal and distal monolayers, they used various types of *immobile* monolayers (either covalently anchored or coupled with an ion bridge) and transferred distal monolayers from the air/water interface. Here, the viscosity of a monolayer of $\eta_m = 0.08$ nN m^{-1}s can be assumed to be one-half of that of a free lipid bilayer ($\eta_{bl} = 0.16$ nN m^{-1}s).[37] Although the surface pressure at which monolayers are transferred (20 mN m^{-1}) is lower than those known for self-assembled free lipid bilayers (typically 30−40 mN m^{-1})[35,38] and the density of the proximal alkyl chains is not quantitatively defined, they observed clear trends in the diffusion coefficient of lipid probes using FRAP analysis that is similar to what is described here. For example, on a cadmium arachidate monolayer whose alkyl chains have crystalline-like order, the lateral diffusivity of a 1,2-dioleoyl-*sn*-glycero-3-phosphocholine (DOPC) monolayer at $T = 293$ K was found to be $\sim 0.4\ \mu m^2\ s^{-1}$. For other proximal monolayers with unknown alkyl chain densities, typical values of $\sim 1\ \mu m^2\ s^{-1}$ were reported.

Similar to the situation described above, the hydrophobic chains of the polymer cushion are immobile, which enables us to apply the same theoretical approximation (e.g., $\eta_m = {}^1/_2\ \eta_{bl} = 0.08$ nN m^{-1}s). However, in contrast to previous work, the lateral diffusion coefficient of an SOPC monolayer on a polymer cushion ($D = 3.2 \pm 0.10\ \mu m^2 s^{-1}$) is larger by a factor of 3−10. Because the chain melting temperatures of dioleoyl chains (−18 °C for DOPC)

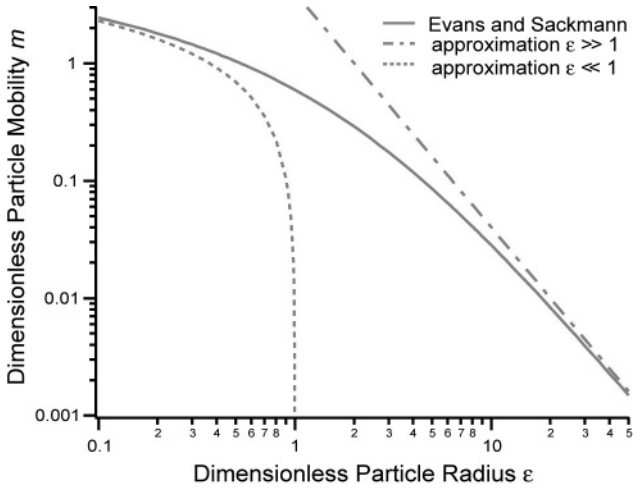

Figure 3. Dimensionless particle mobility m plotted as a function of dimensionless particle radius ϵ, which can be derived using eqs 3−5. From the dimensionless particle mobility calculated from the diffusion constant, one can analytically determine the dimensionless particle radius ϵ.

Table 2. Summary of the Calculated Dimensionless Particle Mobility, Dimensional Particle Radius, and Frictional Coefficient for Lipids and Proteins[a]

sample	dimensionless particle mobility, $m = 4\pi\eta D/kT$	dimensionless particle radius ϵ	frictional coefficient b (N s m^{-3})
Texas red lipid	0.80	0.73	2.0×10^8
His-EGFP	0.37	1.27	5.2×10^8
His-DsRed tetramer	0.35	1.31	5.5×10^8

[a] Diffusion coefficients presented in Table 1 and the viscosity of a monolayer of $\eta = 0.08$ nN m^{-1} s (one-half of that of a free lipid bilayer $\eta_{bl} = 0.16$ nN m^{-1} s[37]) are used to calculate the dimensionless mobility m with eq 7. Using this value, the dimensionless particle radius ϵ can be obtained analytically from Figure 3. It should be noted that the frictional coefficient for proteins ($b = b_s + b_\infty$) includes the additional contribution from drag with the semi-infinite solution b_∞.

(37) Kühner, M.; Tampé, R.; Sackmann, E. *Biophys. J.* **1994**, *67*, 217.
(38) *Phospholipids Handbook*; Cevc, G., Ed.; Marcel Dekker: New York, 1993.

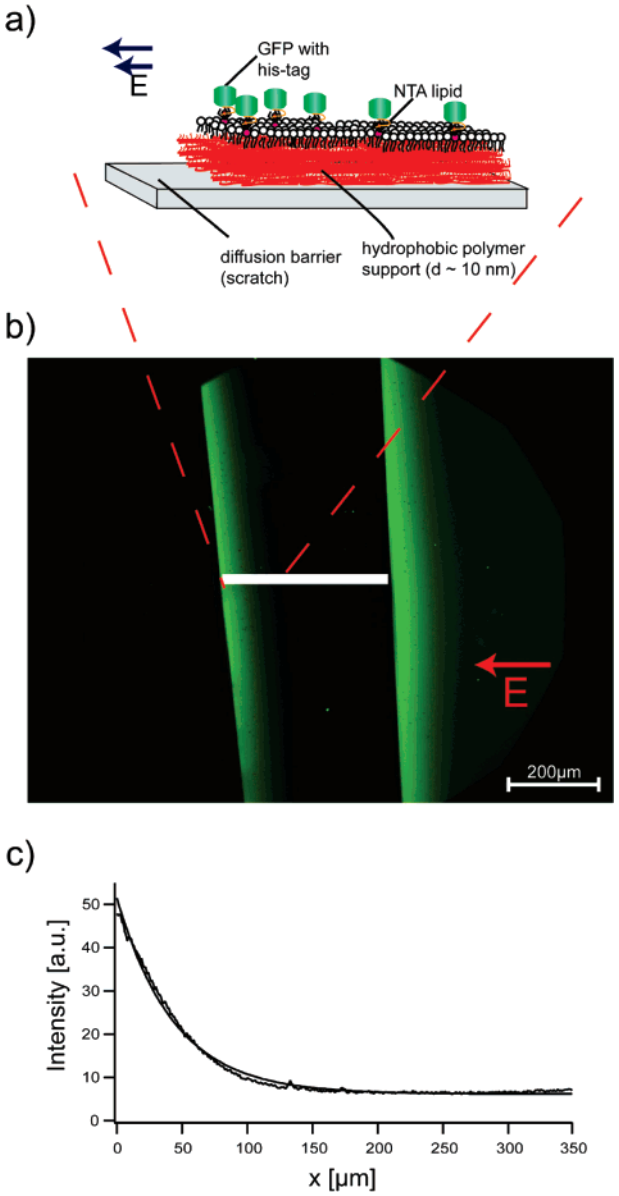

Figure 4. (a) Schematic view and (b) fluorescence image of the static concentration gradient of membrane-anchored His-EGFP (average area per protein of ~40 nm^2), which can be reached by application of a tangential electric field of 10 V/cm for 1 h. (c) Empirical analysis of the 1D intensity profile enabling us to deduce a characteristic decay length of $\xi = 0.022\ \mu m^{-1}$ and a mean velocity of $\langle v \rangle = 33$ nm s^{-1}.

and SOPC (6.5 °C)[38] are much lower than the experimental temperature ($T = 20$ °C), this difference cannot be attributed to a phase transition. The radius of the transmembrane part of $a \approx 5$ Å can be estimated from the area per lipid molecule in a fluid phase, ~65 Å^2. [35] Figure 3 represents the relationship between the dimensionless mobility m and the dimensionless particle radius ϵ, obtained from eqs 4 and 7. By taking the dimensionless particle mobility of $m = 0.80$ calculated from the experiments, one can analytically obtain the dimensionless particle radius ϵ of 0.72 for lipid molecules. Because the penetration of lipid head groups to the exterior aqueous phase (i.e., the effect of b_∞) is negligible, the frictional coefficient of $b_s = 2.0 \times 10^8$ N m^{-3} s can be calculated from eq 5. For comparison, the corresponding plots based on two extreme situations are also presented. In the case $\epsilon \ll 1$, the solution of Saffman and Delbrück's theory[26] is $m \approx \ln(1/\epsilon)$. However, for $\epsilon \gg 1$, the dimensionless particle mobility showed good agreement with the solution of Hughes et al.,[27] $m \approx 4/\epsilon^2$.

Table 3. Summary of the Characteristic Decay Length and Drift Velocity Calculated for Lipids and Proteins

sample	characteristic decay length ξ (μm^{-1})	mean drift velocity $\langle v \rangle$ (nm s^{-1})
Texas red lipid	0.018	58
His-EGFP	0.022	33
His-DsRed tetramer	0.014	22

In comparison to the previous study that utilized the transfer of distal layers,[21] the lateral density of lipids in monolayers prepared by the solvent-exchange method seems to be larger because our membrane preparation relies on the self-assembly of lipids that results in a surface pressure of 30−40 mN m^{-1}. In fact, previous electrochemical characterization confirmed the formation of a highly packed lipid monolayer on the same polymer cushion formed by solvent exchange, without any contamination with residual organic solvent.[25] Despite the higher lateral density, the dimensionless particle radius ϵ and the frictional coefficient b_s on polymer supports are clearly smaller than those reported on crystalline-like alkyl chains.

The diffusion constants of proteins ($D = 1.5 \pm 0.1\ \mu m^2$ s^{-1} for His-EGFP and $1.4 \pm 0.05\ \mu m^2$ s^{-1} for His-DsRed) are almost identical, suggesting that the frictional drag that these different proteins experience in polymer-supported membranes is comparable. Because the frictional drag and the resulting diffusion coefficient scale with the square of the particle radius, as implied by eqs 3−5, the estimated diffusion constants of proteins indicate that the frictional drag from the semifinite bath solution b_∞ (eq 6) is not dominant. This can be understood by the fact that the proteins are not integrated into lipid membranes but are docked to anchoring lipids. Furthermore, this finding clearly indicates that His-DsRed tetramers are coupled to the membrane with one histidine tag and not with four, which also seems reasonable from the structure of DsRed.[39]

As presented in Table 1, the diffusion coefficients of the tethered proteins are smaller than those of lipids by a factor of about 2. However, the size difference between NBD and recombinant proteins is too large to account for this difference only in terms of the frictional drag from the semifinite bath solution b_∞, although the viscous environment around the proteins protruding out of the membrane surface might be different from that of NBD dyes coupled to the lipid head group (Figure 1). Furthermore, the coupling of histidine tag to the NTA head group, which is not separated from the alkyl chain region via any spacer, might cause additional frictional drag. Therefore, because it is not possible to separate these two contributions quantitatively, we calculate here the apparent frictional coefficients $b = b_s + b_\infty$ and approximate the radius of the membrane-inserted part as being comparable to that of a lipid anchor, $a_p \approx 5$ Å. Here, the frictional coefficient of His-EGFP, $b = 5.2 \times 10^8$ N m^{-3} s, was found to be almost identical to that of His-DsRed, $b = 5.5 \times 10^8$ N m^{-3}s, despite the difference in the molecular weight (Table 2). Such a trend observed here—slower diffusion is independent of the size of the tethered object—has also been observed for the tethered vesicles, suggesting that these tethered objects (in the case of tethered vesicles, the size is much larger than that of the proteins, and the tether length amounts to up to 8 nm) can interact with the supporting membrane. Further study with fluorescence

(39) Vogel, M.; Vorreiter, J.; Nassal, M. *Proteins: Struct., Funct., Bioinf.* **2004**, *58*, 478.

Scheme 1. Comparison of (a) a Conventional Solid-Supported Lipid Bilayer and (b) a Polymer-Supported Lipid Monolayer of the Type Used in This Work[a]

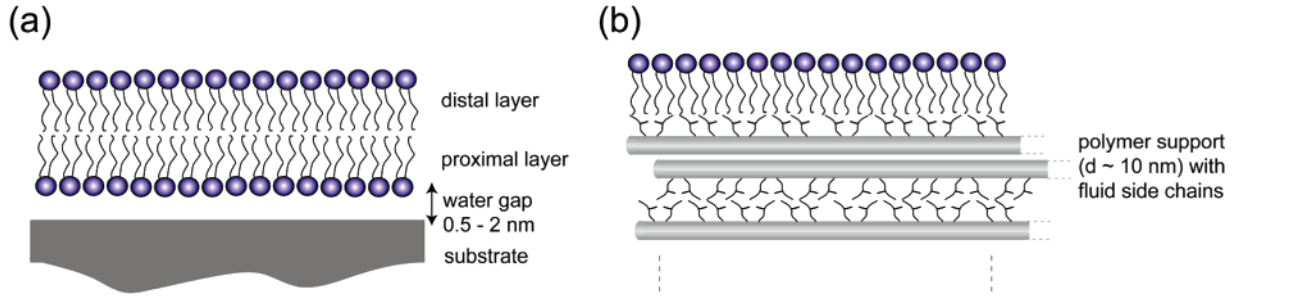

correlation spectroscopy[40] or single-particle tracking[41] would allow for the discrimination of the different modes of lateral diffusion on various length scales, such as solvent caging and site jumping.

Thus, we conclude that the isopentyl side chains of IPCC polymer supports can provide distal lipid monolayers with less interfacial friction, which leads to the higher lateral diffusivity of lipids and lipid-anchored proteins. As described by eqs 3−7, the increase in the diffusion coefficient by the reduction of frictional drag should also facilitate an increase in electrophoretic mobility, which enables the effective accumulation of lipids and proteins, and this is described in the next section.

Electrical Manipulation of Lipids and Anchored Proteins. As depicted schematically in Figure 4a, His-EGFP coupled to a polymer-supported lipid monolayer (SOPC monolayer with 2 mol % NTA-DOGS, which is the same membrane as presented in Figure 1) can be driven toward the negative electrode (i.e., these anchored proteins move in the direction of the field). After 1 h, the concentration gradient reaches steady state, and an epifluorescence image is shown in Figure 4b and a line profile of the intensity is shown in Figure 4c. An empirical analysis of the steady-state concentration gradient with eqs 1 and 2 yields the solid curve in Figure 4c and the characteristic decay length of $\xi = 0.022\ \mu m^{-1}$. Taking the passive diffusion coefficient from FRAP measurements, $D = 1.5 \pm 0.1\ \mu m^2 s^{-1}$, the mean drift velocity can be calculated to be $\langle v \rangle = 33\ nm\ s^{-1}$. His-DsRed tetramers coupled to the same polymer-supported monolayer (SOPC monolayer with 2 mol % NTA-DOGS) also accumulate in the same direction as His-EGFP upon application of an electric field. By taking the lateral diffusion coefficient of His-DsRed, $D = 1.4 \pm 0.05\ \mu m^2\ s^{-1}$, the same empirical analysis yields $\xi = 0.014\ \mu m^{-1}$ and $\langle v \rangle = 22\ nm\ s^{-1}$. The calculated values are summarized in Table 3.

Interplay of Electrophoresis and Electroosmosis. Texas red- and NBD-labeled lipids, which carry one negative charge per molecule, accumulate toward the positive electrode, as expected if their motion is dominated by electrophoresis.[11,12] Quantitative analysis of the Texas red gradient profiles yield a characteristic decay length of $\xi = 0.018\ \mu m^{-1}$ and a mean drift velocity of $\langle v \rangle = 58\ nm\ s^{-1}$. By contrast, His-EGFP and His-DsRed are observed to move in the direction of the electric field, although the isoelectric points of these two proteins ($pI_{His-EGFP} = 4.8 - 5.0$ and $pI_{His-DSRed\ tetramer} = 7.2 - 7.4$) indicate that they should carry net charges of opposite signs under the experimental condition of pH ~5.5. [To determine the isoelectric point (pI) of His-EGFP and His-DsRed, we carried out gel isoelectric focusing (IEF) experiments. A Pharmacia LKB system and slab gels with a 3.0−9.0 pH gradient were used for IEF. The system was calibrated with the 3.6−9.3 IEF mix from Sigma-Aldrich, yielding $pI_{His-EGFP} = 4.8-5.0$ and $pI_{His-DSRed\ tetramer} = 7.2-7.4$. The value of His-EGFP agrees well with the value reported by Richards et al.[42] Because all of the electric manipulations were carried out in Millipore water (pH ~5.5), we can assume that His-EGFP carries negative charges, and the His-DsRed tetramer carries positive charges.] Similar results were reported for lipid-tethered proteins[34] and vesicles,[15,16] suggesting that the protein is driven not only by electrophoresis but also by the force from the bulk flow of ions (electroosmosis).

Scheme 2. Schematic Illustration of the Interplays of Various Forces

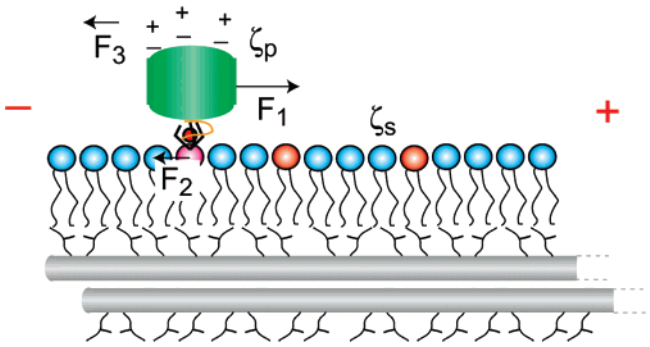

Here, the steady state, at which the proteins are drifting at a constant velocity v_1, can be reached if the Stokes force acting on the sphere of radius R is balanced by the force on the plane of shear and the drag force acting from the lipid anchor (with a radius of $a_p \approx 5$ Å)[18]

$$6\pi\mu_{H_2O}R(v_1 - v_2) = 6\pi R\epsilon_1\epsilon_0\zeta_p E - 6\pi M_m a v_1 \qquad (8)$$

μ_{H_2O} is the viscosity of water, and $M_m \approx 0.03\ N\ m^{-2}\ s$ is the bulk viscosity of a lipid membrane (i.e., not the 2D viscosity used in eqs 4−7). The velocity of a fluid adjacent to the membrane surface v_2 (i.e., outside the electric double layer), which can be described by the Helmholtz-Smoluchowski equation, is

$$v_2 = \frac{\epsilon_1\epsilon_0\zeta s}{\mu_{H_2O}} \qquad (9)$$

ϵ_1 is the dielectric constant of the aqueous phase (~80), ϵ_0 is the permittivity of free space, and ζ_s is the zeta potential (the potential at the plane of shear, where $v = 0$) of the surface. The mean value of the velocities of individual proteins (v_1) is the mean velocity that can be analytically obtained from the protein gradient; therefore, the effective electrophoretic mobility u can be calculated

(40) Zhang, L.; Granick, S. *Proc. Natl. Acad. Sci. U.S.A.* **2005**, *102*, 9118.
(41) Qian, H.; Sheetz, M. P.; Elson, E. *Biophys. J. 60*, 910.
(42) Richards, D.; Stathakis, C.; Polakowski, R.; Ahmadzadeh, H.; Dovichi, N. J. *J. Chromatogr., A* **1999**, *853*, 21.

as

$$u = \frac{v_1}{E} = \frac{\epsilon_1\epsilon_0(\zeta_p - \zeta_s)R}{\mu_{H_2O}R + \mu_m r} \quad (10)$$

The fact that both positively and negatively charged proteins are driven toward the negative electrode suggests that the contribution of electrophoresis is rather minor compared to the electroosmotic flow, whose magnitude scales linearly with the zeta potential of the supported membrane surfaces. [We observed no effect of the surface charge density on the diffusion coefficients and mobile fractions of His-EGFP within the experimental error.] In fact, the drift velocities of His-EGFP measured on the supported membranes with negatively charged SOPS lipids scale almost linearly with the fraction of negatively charged lipids, as predicted by eq 10. A systematic analysis of the balance between electrophoresis and electroosmosis was recently described using lipid vesicles tethered on supported lipid membranes, where the charge on the supporting bilayer and tethered vesicle can be independently and widely varied.[16]

Although it is difficult to calculate the zeta potentials quantitatively under such salt-free conditions, the observed tendency strongly supports our hypothesis and further suggests the potential of regulating protein drift velocities by adjusting the interplay between electrophoresis and electroosmosis.

Conclusions

We demonstrate that polymer-supported monolayers can be used to tether His-tagged proteins to Ni-NTA lipids under conditions where the proteins exhibit good lateral mobility and that it is possible to manipulate these anchored proteins electrically. The surface density of proteins can be optimized (40 nm^2/protein) to avoid nonspecific protein adsorption and 2D crystallization, which provide proteins with a fluid environment for free lateral diffusion. From the diffusion coefficient obtained by FRAP measurements, one can quantitatively determine the frictional drag acting at the protein−membrane interface. The application of a tangential electric field to the mobile proteins anchored on a patterned surface leads to an accumulation of proteins, resulting in a steady-state concentration gradient. An analytical solution of the steady-state gradient shape yields the mean velocity of lipids/proteins. As suggested by previous work on cell membranes[18] and tethered lipid vesicles,[16] the mean velocity of anchored proteins depends on the membrane surface charges (i.e., zeta potential difference between proteins and the membrane surface). The system established here can be used for physically modeling the interplay of the work of many sorts of fluxes on cell surfaces as well as for local functionalization of solid surfaces with the gradient of membrane-anchored proteins with different net charges.

Acknowledgment. We thank F. Rosell, J. M. Johnson, C. Yoshina-Ishii, R. Tampé, V. Kahl, O. Purrucker, S. G. McLaughlin, and E. Sackmann for helpful discussion. This work was financially supported by DFG (SFB 563 C6, Ta 259/5) and Fonds der Chemischen Industrie (to M.T. and M.F.) and by grants to S.G.B. from the NIH (GM069630), the NSF biophysics program, and the MRSEC program of the NSF under award DMR-0213618 (CPIMA).

Supporting Information Available: Cloning of His-EGFP and His-DsRed and expression and purification of oligohistidine-tagged fluorescent proteins. This material is available free of charge via the Internet at http://pubs.acs.org.

LA0628219